Mining
Mineração

Unplanned dilution back analysis in an underground mine using numerical models

http://dx.doi.org/10.1590/0370-44672021750093

Diogo Peixoto Cordova[1,3]
https://orcid.org/0000-0002-0985-7962
André Cezar Zingano[2,4]
https://orcid.org/0000-0002-3740-9104
Ítalo Gomes Gonçalves[2,5]
https://orcid.org/0000-0002-5546-6102

[1]Universidade Federal do Pampa - UNIPAMPA, Campus Caçapava do Sul, Caçapava do Sul – Rio Grande do Sul - Brasil.

[2]Universidade Federal do Rio Grande do Sul – UFRGS, Departamento de Engenharia de Minas Porto Alegre – Rio Grande do Sul - Brasil.

[3]Universidade Federal do Pampa - UNIPAMPA, Campus Caçapava do Sul, Caçapava do Sul – Rio Grande do Sul - Brasil.

E-mails: [3]diogocordova@unipampa.edu.br, [4]andrezin@ufrgs.br, [5]italogoncalves@unipampa.edu.br

Abstract

In underground mines, stability problems can cause unplanned dilution, increasing the costs of mining operations, such as loading, transport, crushing and grinding. This is usually dealt with by simply increasing investments with support. However, the design geometry of stopes and drifts also has a great effect on a stope's stability. The use of empirical stability methods is a very common practice, however because of their few input parameters, it cannot predict the actual performance related to each stope and drift design. This study has as main goals a back analysis of the actual dilution, using the Equivalent Linear Overbreak Slough (ELOS) method and analysis in the drift developments at the hanging wall contact, using numerical models. The case study is an underground hard rock gold mine, with a pillar-less Transversal Stope method. The hanging wall failure was quantified using a database from 19 stopes measured by the Cavity Monitoring System (CMS). Numerical finite elements models (FEM) were used, and 5 primary stopes were selected to calibrate models. The volumes of actual dilution showed a good correlation with the volumes of the relaxation zones produced by the models. Then, new optimized drift geometry layouts at the hanging wall contact were proposed, showing a decrease in 2.35 times in the relaxation zone of the numerical models, therefore justifying the use of these models as a dilution optimization tool. This methodology also proved to be useful in the definition of cable bolt length.

keywords: unplanned dilution, transversal stopes, hanging wall, cable bolts, ELOS.

1. Introduction

In an underground mine, stability problems can cause dilution. This can be attributed to the rock mass quality and stress state, in addition to the stope and drift geometries. Efforts to reduce unplanned dilution require an understanding of all those factors that directly and indirectly affect the entry of waste material into stopes.

The 1970s saw the development of the first empirical systems for underground excavation stability, the RMR system (Bieniawski, 1973, 1989; Celada *et al*., 2014) and the Q System (Barton *et al*., 1974; Grimstad and Barton, 1993; Barton and Grimstad, 2004). These systems, initially more applied when excavating civil tunnels, allowed the definition of the need for rock mass support and the maximum dimensions in unsupported spans.

Mathews *et al*. (1981) create an empirical method aimed at the stability of underground stopes. Over time this method has been adapted by different authors (Potvin, 1988; Nickson, 1992; Mawdesley *et al*., 2001) seeking to increase its reliability in the dimensioning of stable stopes supported with cable bolts. This graphical method uses the modified stability number (N'), which depends on modified Q (Q'), versus hydraulic radius (HR). Melo *et al*. (2014) has verified the applicability of empirical methods in contexts of Brazilian underground mines, showing a lack of site-specific studies. Santos *et al*. (2020) proposed a methodology using neural networks to assess the open stope stability using local stope data of a Vertical Retreat Mining (VRM) method.

Modern rock mechanics is heavily grounded in the use of numerical modeling software to complement and verify traditional empirical methods, as demonstrated by Zingano *et al*. (2007), Napa-García *et al*. (2019), Abdellah *et al*. (2020), and Hefni *et al*. (2020). Numerical modeling allows investigating the complex behavior of excavations, analyzing the interactions and deformations caused between excavations and stress redistributions, through computational applications. Systems of partial differential equations are used to describe the analyzed model. The software implements the equations for the finite element method (FEM), finite difference method (FDM), among others. The models represent the system geometry, boundary conditions, in-situ stresses, constitutive model and failure criteria. Numerical modeling techniques can also include time effects, excavation sequence, and the interactions between excavations and fault or discontinuity interfaces.

The initial objective of this study is to quantify the existing dilutions in a case study of an underground gold mine, which uses backfilling in the Transversal Stope mining method. The main objective of this study is the use of numerical models that can represent the existing scenario, justifying the use of these models as an optimization tool for dilution, considering drifts excavations and cable bolt lengths.

2. Material and methods

2.1 Dilution

There are two concepts of dilution, planned dilution and unplanned dilution. Internal planned dilution occurs due to the presence of waste inclusions, in the form of thin lenses, and thus, they cannot be effectively separated as waste during mining. However, this dilution is already included in the resource estimate. Otherwise, unplanned dilution can be caused by overbreaking or slough of the hanging wall (HW), during the mining of the stopes (Scoble and Moss, 1994).

There are several methods for dilution calculation. Clark and Pakalnis (1997) used the overbreak volume and the size of the HW stope surface as a measure of stope performance, defining the ELOS (linear equivalent over-break/slough). Clark (1998) incorporated to the modified stability graph method an empirical estimation of overbreak/slough considering the ELOS factor. Equation 1 below defines the ELOS.

$$ELOS = \frac{V_{OB}}{A_S} \tag{1}$$

Where V_{OB} is the overbreak volume, and A_S is the exposed surface area of the HW. Table 1 demonstrates the observations, considering the ELOS value obtained from Clark (1998).

Table 1 - ELOS value ranges. Source: Clark (1998).

ELOS	Observation
< 0.5m	Blast damage only
0.5m – 1m	Minor sloughing
1m – 2m	Moderate sloughing
> 2m	Severe sloughing/Wall collapse

Henning and Mitri (2007) developed, analogously to ELOS, the dilution potential from a 3D numerical model, where the boundary of the dilution is represented by the minor principal stress isoline, equal to zero (σ_3 = 0 MPa). The term dilution density (DD) was used, and its measurement unit was in meters. This allows estimating the likely slough of any of the walls of the stope. Equation 2 below defines the DD.

$$DD = \frac{\text{unplaned dilution volume } (m^3)}{\text{exposed wall surface area } (m^2)} \tag{2}$$

2.2 Stress state

In mining engineering, *in-situ* stresses control the distribution and magnitude of stresses around underground excavations, such as in tunnels, raises, galleries, wells and stopes (Hoek and Brown, 1980). In general, stress-related stability problems increase with depth, but can also be encountered in shallow excavations due to high horizontal *in-situ* stresses. The orientation and magnitude of in-situ stresses affect the planned geometry, excavation sequence, and orientation of underground excavations (Amadei and Stephansson, 1997).

During the development of drifts, there are crucial points where large stress-induced changes occur. One of these points is precisely in the contact between the lower-level stope drift (undercut) and the HW. At this point, the undercut produces an increase in the relaxation zone, where stresses are close to zero and tangential to the HW. Thus, dilution occurs when the minor principal stress (σ_3) is equal or less than zero (Diederichs and Kaiser, 1999; Martin *et al.*, 1999; Wang, 2004).

2.3 Numerical modeling

The main application of numerical methods in mining is basically to provide an analysis of the changes in stress, strain and displacement induced by the excavation process. Such information is a guide for assessing the stability, safety and economics of underground excavation projects. Jing and Hudson (2002) and Brady and Brown (2005) present the basic principles of numerical methods and their applications in rock mechanics. Each method has its specific characteristics and is applied depending on the problem. Problems in rock mechanics can be summarized in two types: continuous and discontinuous.

Assuming that the rock mass is fractured, constituted by different rock properties and blocks limited by fractures, it can be said that the rock mass is heterogeneous and discontinuous. When these elements are of small size, compared to the characteristics and size of the excavation and the geomechanical model, the blocks will not be the cause of failures or preferential planes of deformations. So, in this case, the rock mass can be treated as a continuous and homogeneous medium, within the same type of rock (Zhu and Wang, 1993).

In the finite element method (FEM) the entire problem domain is divided into small regions containing non-overlapping elements, which are connected to each other through points called nodes. As the domain division can be any, this method has a great advantage in handling cases with complex geometry (Jing and Hudson, 2002). The FEM is a popular method for modeling engineering problems, even though it requires some computational power, as a great number of partial differential equations need to be solved (Pariseau, 1993).

3. Case study

3.1 Geology

The deposit develops along a shear zone with a main NW-SE direction and a dip varying between 45 and 70 degrees south. The orebody is approximately 750 m along the east-west axis and 750 m along with the dip. Intense hydrothermal alteration processes, associated with brittle-ductile deformation, affect monzonitic rocks, generating highly deformed hydrothermalites.

These processes are mainly related by two first-order mine-scale faults: H1, corresponds to the upper limit of the hydrothermal zone (hanging wall), with a width between 2-8 m and F1, corresponds to the base of that zone (footwall); the width of this zone varies between 60-100 m. A third fault (NW), plunging approximately 30° SW controls the immersion axis of the mineralization (Figure 1).

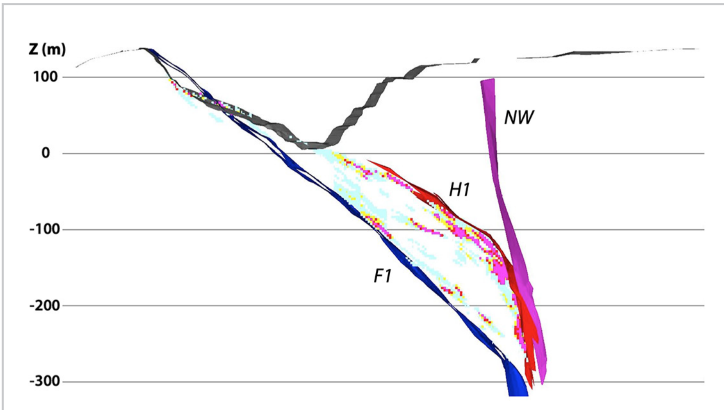

Figure 1 – Cross-section of the ore zone, looking east, showing the main faults.
The H1 fault corresponds to the upper limit of the hydrothermal zone (hanging wall);
the F1 fault corresponds to the base of that zone (footwall); and the NW fault controls the immersion axis of the mineralization.

3.2 Mining methods

Initially, the deposit was mined by open pit, being later in 2010 mined underground until 2016. The main Portal was developed in the bottom of the open pit, level -7 m. The underground mine used two mining methods, Inclined Room and Pillars (IRP) and Transversal Stopes (TS), which will be the object of this study. The TS method was used to extract the largest mineralized zone, located below level -120 m. This method is a transverse variation of the Sublevel Stope method, which consists of extracting the ore forming large open stopes separated by sub-levels, the undercut and overcut. The longest axis of the stope is perpendicular to the strike of the ore body. The draw points are located at the undercut drifts and extend from the HW to the FW. This method requires more waste development on the footwall and is generally used when the quality of the HW limits the span of the stopes. However, it allows for greater flexibility to mining sequences.

The drift excavation begins in the FW and goes to the HW, reaching as close as possible to the fault zone, where the highest grade is. The drift excavation gallery consists of a 5 × 5 m semicircular arc section. Each round has 3 m of advance rate, using the conventional drill and blast method. Regularly spaced split sets are used as primary support.

Initially, between levels -182 m and -220 m, the TS method was used, keeping pillars about 8 m wide between the extracted stopes. After being extracted, the stopes were filled with waste rock (Uncemented Rock Fill – URF). The stopes had 20 m high, 20 m wide and a variable length between 20 m to 50 m. Considering a modified stability number (N') of 1.65 and a hydraulic radius (HR) of 5.66, the empirical method (Potvin, 1988) suggested the use of 9 m cable bolts.

During the mine's operation, an economic feasibility study showed an opportunity to change the method, where a pillar-less method was adopted. This was possible using a mixture of cement and waste rock (Cemented Rock Fill - CRF) for the primary stopes, and URF backfilling for the secondary stopes. This method was used between levels -120 m and -182 m with the mining sequence shown in Figure 2. The extraction sequence starts with the primary stopes in the lower level in ascending mining sequence. The extraction of the secondary stopes begins, as soon as the adjacent stopes, filled with CRF, reach the required curing period.

Figure 2 - Complete extraction sequence of the Transversal Stopes method with CRF and URF filling types (Cross-section looking North).

3.3 Rock mass properties

The geomechanical review was obtained by the company, with the support of external consulting. The rock mass properties were defined based on the combination of geomechanical descriptions of 59 oriented boreholes totaling 7.176 m of rock cores, laboratory strength tests (66 UCS tests, 26 Brazilian tensile tests, 36 triaxial compression tests and 24-point load tests). The generalized Hoek-Brown failure criterion (Hoek *et al.*, 2002) and the elastic parameters are shown in Table 2.

Table 2 - Geomechanical parameters of the rock mass.

Parameters	Ore	HW	FW	H1	F1
Young's modulus	50.9 GPa	21.9 GPa	44.1 GPa	3.9 GPa	7.7 GPa
Poisson's ratio	0.20	0.23	0.21	0.27	0.26
Density	2.73 t/m^3	2.75 t/m^3	2.63 t/m^3	2.73 t/m^3	2.80 t/m^3
GSI	70	55	65	40	45
mb parameter	4.17	1.83	2.48	0.12	1.36
s parameter	0.036	0.007	0.020	0.001	0.002
a parameter	0.5	0.5	0.5	0.5	0.5

3.4 In-situ stress

To date, there are no studies published or carried out in the region regarding the measurement of *in-situ* stress. Thus, it was considered that σ_1 is contained in the horizontal plane (north-south trend 15°), perpendicular to the mineralization plane. The σ_2 is also contained in the horizontal plane, but parallel to the mineralization plane (east-west) and the σ_3 is vertical.

The magnitude of the stresses was assumed considering that the geological environment is relatively stable and far from important tectonic influences. For the vertical stress (σ_v), Equation 3, obtained by Brown and Hoek (1978) was used, which uses the mean value of the specific weight of 0.027 MN/m^3 (very close to the specific weight of the site lithologies). The horizontal stress component (σ_h) is calculated by Equation 4, using a k factor multiplied by the σ_v.

$$\sigma_v = 0.027z \tag{3}$$

$$\sigma_h = k\sigma_v \tag{4}$$

Where the value of k was obtained using the thermal elasto-static Earth model developed by Sheorey (1994). Equation 5 is shown below:

$$k = 0.25 + 7E_h\left(0.001 + \frac{1}{z}\right) \tag{5}$$

In this equation, z is the depth (m) below the surface and E_h is the average of the deformation modulus of the upper portion of the earth's crust. Thus, considering an average deformation modulus of about 20 GPa and an average depth of

300 meters, the value of k equal to 1.5 was obtained from the graph. This value was used in the calculation of the maximum horizontal main stress ($\sigma_1 = \sigma_{h1}$). As for the stress σ_2 (σ_{h2}) has set the intermediate value of k_2 equal to 1.2.

4. Methodology

4.1 Stope database

The database used for dilution calculations came from the Cavity Monitoring System (CMS) of 19 stopes extracted from 2013 to mid-2015. The planned geometry of each stope was intersected with the actual geometry, using Boolean operation. After that, the resulting geometry needs to be cut with the HW surface, obtaining the volume and the surface area of the HW dilution, for ELOS calculation.

4.2 Model calibration

The back analysis is the procedure that analyzes field data and calibrates the data entered in the models so that they can be used as a starting point in future models. In order to correctly calibrate the 3D elastic numerical models, it is necessary to use dilution data (ELOS) from selected primary stopes that were mined without the stress influence of near excavations or geomechanical problems, which could bias the results of the dilution density (DD) from numerical models. To create the models by the FEM, the RS3 software developed from Rocscience was used (Rocscience, 2021). The material properties included in the models were those based on the geomechanical characterization study carried out by the company.

The fundamental premise is that the CMS represents the rock mass zones where the failure occurred. However, this can lead to some variations in the results of the analysis, as the CMS scanning profile may show elements of the HW that have suffered failures, but which have not yet been removed, as an artificial arc formed by the cable bolts can maintain these elements in place. Furthermore, errors or deviations in drilling and blast can also influence the dilution. However, as this cannot be confirmed in this study, it must be assumed that the dilution is due to rock mass stress failures. Figure 3 below shows one of the 5 primary stopes used in the calibration, where it is possible to visualize the actual hanging wall dilution and the numerical model with the resulting relaxation zone.

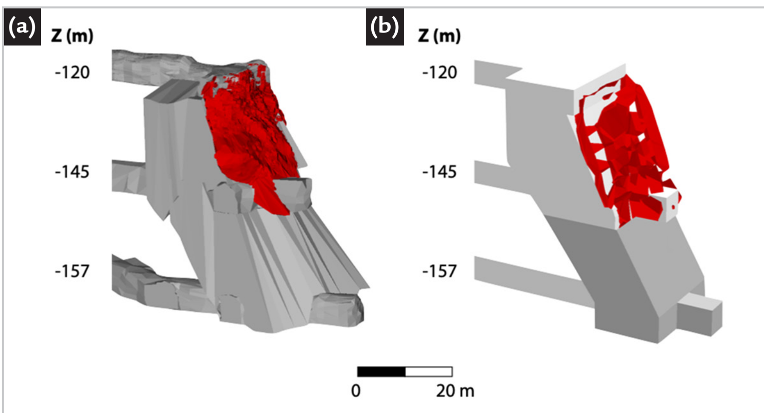

Figure 3 – (a) Actual hanging wall failure in red; (b) Numerical model within the resulting relaxation zone in red.

5. Results and discussion

5.1 Dilution

The stopes from database were classified according to the ELOS classification to obtain linearized dilution values, allowing a direct comparison between different stopes. The results show a major occurrence of severe sloughing in the stopes, with 8 cases with ELOS value greater than 2 m, as shown in the histogram of the Figure 4 below.

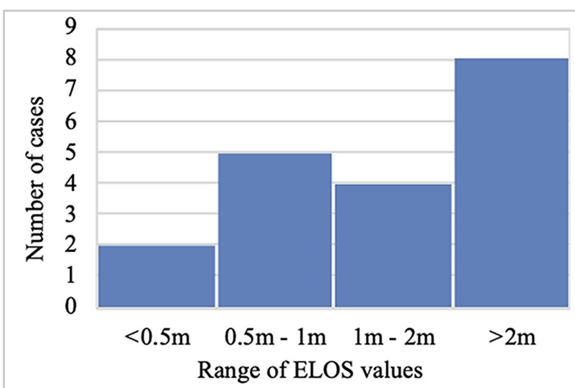

Figure 4 – Histogram of ELOS classification for the analyzed stopes.

5.2 Model calibration

After performing the model calibration for the 5 primary stopes, the DD values were calculated, for this, the relaxation zone volumes ($\sigma_3 \leq 0$) were measured in each scenario and this value was divided by the area of the corresponding HW. The actual dilution values (ELOS) and the DD were plotted on a scatter plot. Linear regression was used to demonstrate the mathematical relationship of actual data versus estimated data. The data correlation coefficient (R^2) of 0.99 demonstrates that there is an excellent data correlation.

Numerical models were also performed with different values of k_1 and k_2 to verify their influence on the model result, since these parameters were defined without the use of real data from *in-situ* stress measurements. The numerical models for the isotropic condition of k_1 and k_2 equal to 1, were less likely to overestimate the dilution values compared to the other values of k_1 and k_2 (Figure 5).

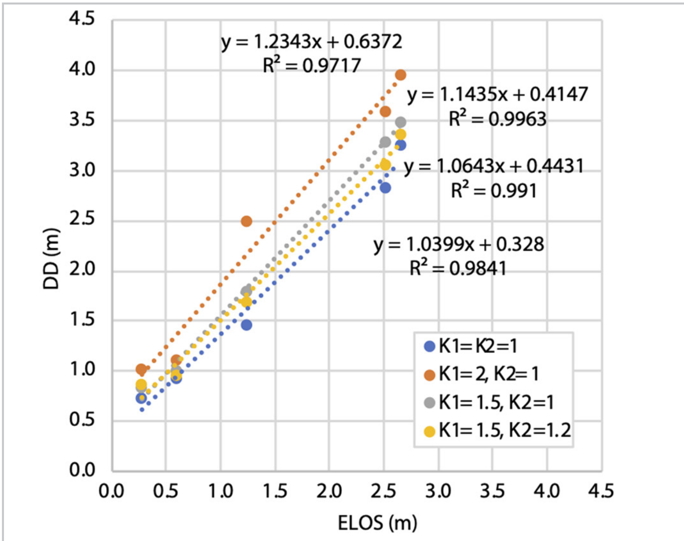

Figure 5 - Scatter plot of DD values plotted against the ELOS value for the five primary stopes chosen, varying the values of k_1 and k_2.

5.3 Influence of drifts over-excavation on dilution

The hanging wall fault zone was previously mapped using surface and underground drill holes. However, only with field mappings did the fault contact become more accurate. Considering that the drift excavation needs to get as close as possible to the fault zone, where the highest grade is, excavating them requires good field control.

Comparative numerical models were produced between cases with and without over-excavation at the HW of both drifts, all properties being equal. The over-excavation considered is of an extra round of 3 m of advance rate, with a 5 × 5 m gallery section. The excavation was made using a full-face drill and blast method, with regular hole depths, without pre-cut, and using ANFO explosives.

The stope size was approximately 25 × 25 × 30 m (height × width × length). A comparison of the σ_3 stress distribution in Figure 6, shows an increase in the relaxation zone in the case with over-excavation, resulting in a large zone of potential instability or dilution. This effect occurs because a hangingwall face interruption is caused by the drift over-excavation, leading to an increase in their exposed area. The calculation of the dilution density shows this increase and can be seen in Table 3.

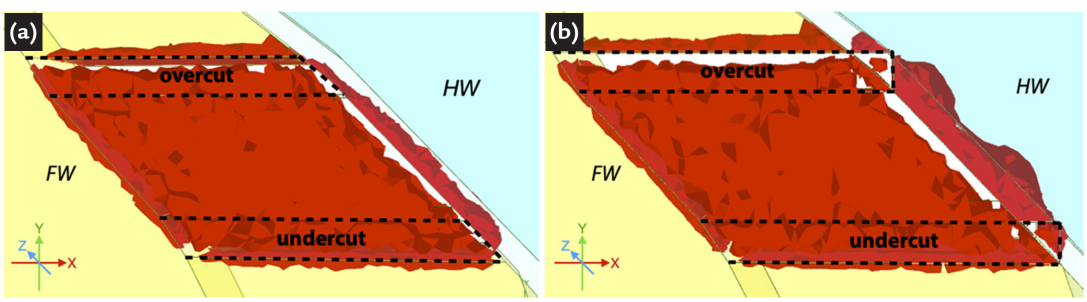

Figure 6 – Cross-section of the $\sigma_3 \leq 0$ isosurface of the numerical model for a planned stope. (a) Without the over-excavation of the undercut and overcut galleries in the HW; (b) With the over-excavation.

Table 3 - Calculation of the dilution density (DD) in both cases.

Models	Relaxation zone m³	Exposed HW m²	DD m
Without over-excavation	883.7	696.2	1.27
With over-excavation	2,073.7	810.6	2.56

As represented by the models, the over-excavation of the HW causes an increase in the stress relaxation zone. This finding actually was observed, for example in the TS-157-W1 stope where both the undercut and overcut drifts crossed the HW fault, causing dilution (Figure 7).

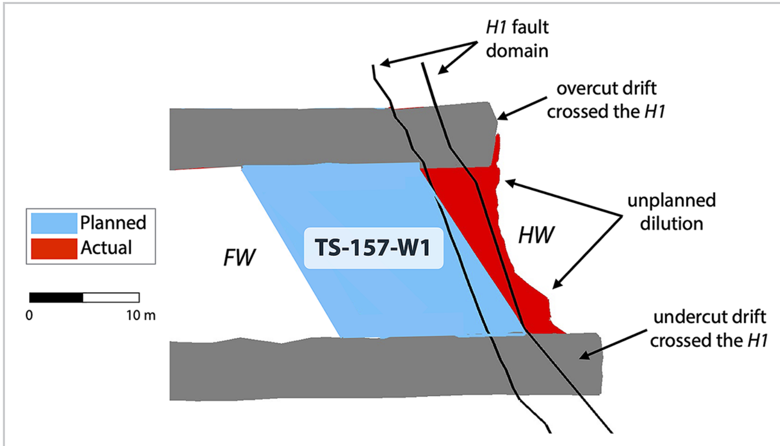

Figure 7 – Actual (TS-157-W1) stope cross-section, comparing the planned design (blue) with the actual geometry from CMS (red), where unplanned dilution can be seen, caused by the development of both overcut and undercut within the fault zone.

5.4 Cable bolt length analysis

Figure 8 below shows the TS-145-W3 and TS-195-W1 stopes cross-sections, with the planned geometry (blue) and actual geometry (red), where undercut and overcut drifts crossed the HW fault, producing a relaxation zone that led to dilution also. It is possible to notice the inefficiency of the cable bolts installed in this zone.

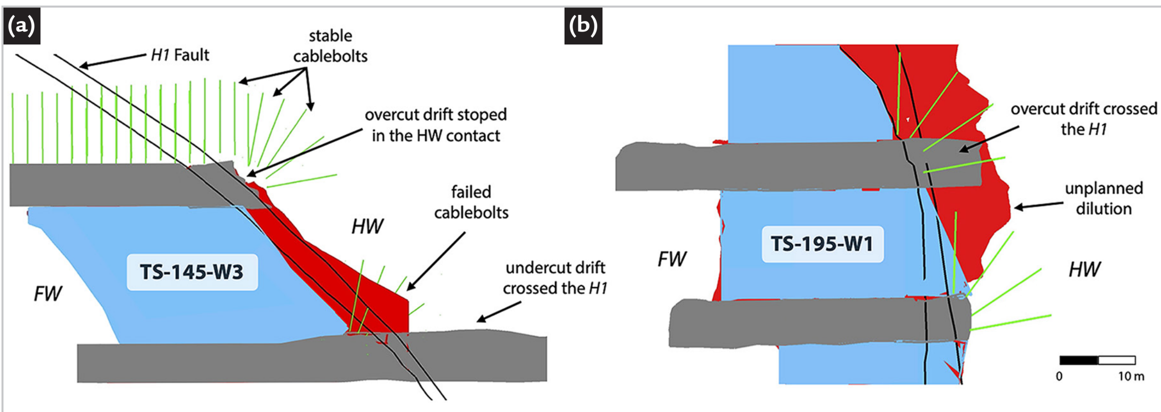

Figure 8 – Actual stopes cross-section comparing the planned design (blue) with the actual geometry (red). We can notice the inefficiency of the cable bolts installed in both stopes. (a) Stope (TS-145-W3) with undercut over-excavation; (b) Stope (TS-195-W1) with overcut over-excavation.

In Figure 9, the numerical models produced considering the over-excavation of drifts, show that the 9 m cable bolts in the middle of the hanging wall are anchored, almost entirely, within the stress relaxation zone, which is not recommended, since this is where the cable bolts have less strength at the cement-cable interface. The solution would be using longer cable bolts, around 15 m to ensure an anchorage greater than 2 m outside the relaxation zone limit, as shown by Hutchinson and Diederichs (1996).

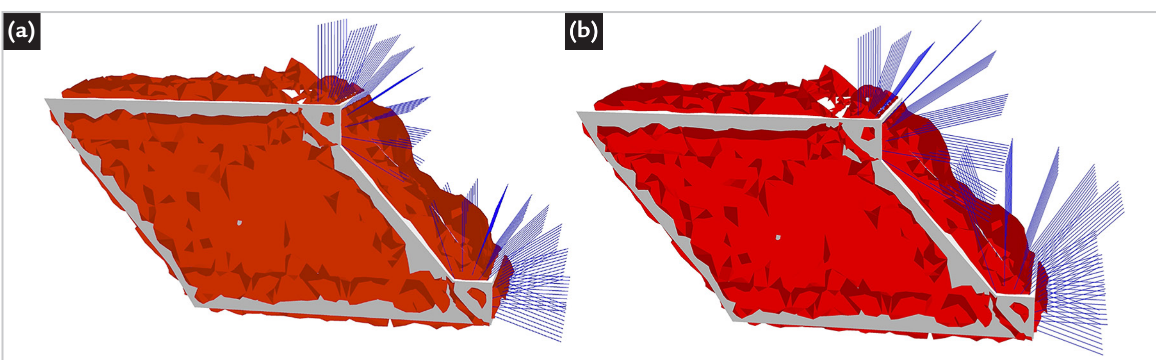

Figure 9 – Perspective view with the $\sigma_3 \leq 0$ isosurface of the numerical model for a planned stope with both overcut and undercut drifts over-excavation: (a) Stope with 9 m cable bolts; (b) Stope with 15 m cable bolts in the hanging wall center.

5.5 Stope location influence

Another six models were produced with different stope locations, to analyze the effect of local stope sequence in the relaxation volume zone, as Henning and Mitri (2007) have already shown in theory. The models considered the drifts over-excavation. The first model was the isolated stope, considered the base case. The other cases were: one adjacent stope mined; both sides mined; one side and below mined; both sides and below, and below only. These findings show that when sides are already mined, the hanging wall of the planned stope will have an increase in the volume of relaxation, because of the change in stress path by the generated voids, that is stress redistribution. The worst case, with both sides mined, shows a 20% increase in DD when compared to the base case. The one side mined scenario shows a 17% increase. Figure 10 shows the simulated scenarios and the respective DD.

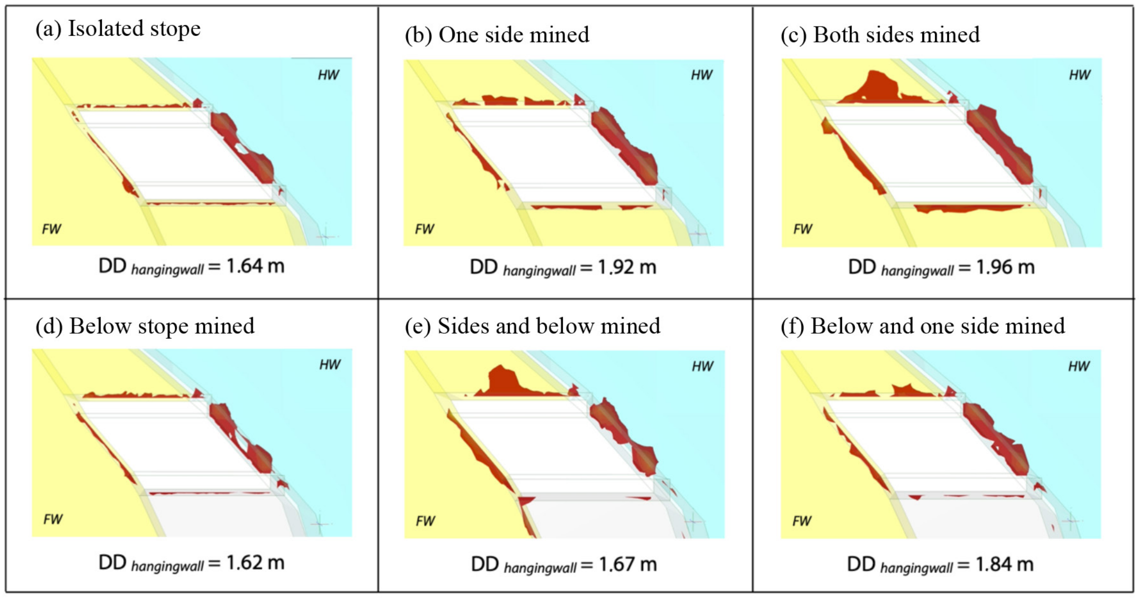

Figure 10 – Simulated scenarios of expected DD related to the stope location and surroundings.

6. Conclusion

The calibrated 3D elastic models allowed us to confirm that the *in-situ* stress considered produced numerical models with a good correlation between the modeled dilution (DD) and the actual dilution, measured by the ELOS factor. There was a slight tendency to overestimate the dilution obtained through the models, even when considering an isotropic stress state. This probably was due to the small tensile strength of the rock mass and the cable bolts installed in the hanging wall, providing even if low, a certain efficiency in containing the rocks in the relaxation zone. These calibration models also show that when the σ_h *in-situ* stress increases, the volume of the relaxation zone in the hanging wall also increases. This is naturally observed near surface excavations, where the *k* factor is higher. The stress redistribution caused by the excavations of adjacent stopes also affects the relaxation zone, increasing it by 20%, as observed in the models produced.

The over-excavation of only 3 m through the hanging wall by both drifts, can lead to a 2.35-times increase in the volume of the relaxation zone and a correlated increase of 2 times in the DD. Thus, the drift over-excavation must be minimized with better field control by the geomechanics department when developing drifts near the hanging wall, avoiding crossing the hanging wall fault as much as possible.

The main limitation of the empirical methods for stability analysis and dilution estimation is that they are limited to the database of cases and that can bias the results in sites where there is a lack of data. These methods also do not consider the relaxation zone around the stopes, thus the effect of the presence of adjacent stopes already mined and the over-excavation of drifts into the hanging wall.

The elastic numerical model demonstrates that the length of the cable bolts on the hanging wall must be defined to ensure that they are anchored outside the relaxation zone in each case. Thus, the best design flow of new stopes should start with stability analysis and dilution estimation by empirical methods. Afterwards, it is convenient to use a numerical model to better estimate the actual dilution and optimize the design.

Acknowledgments

The authors wish to thank UFRGS and UNIPAMPA for their support in this research.

References

ABDELLAH, W. R. E.; HEFNI, M. A.; AHMED, H. M. Factors influencing stope hanging wall stability and ore dilution in narrow-vein deposits: Part 1. ***Geotechnical and Geological Engineering***, v. 38, n. 2, p. 1451–1470, 2020.

AMADEI, B.; STEPHANSSON, O. ***Rock stress and its measurement***. London: Chapman & Hall, 1997. 490 p.

BARTON, N.; LEIN, R.; LUNDE, J. Engineering classification of rock masses for design of tunnel support. ***Rock Mechanics***, v. 6, n. 4, p. 189–236, 1974.

BARTON, N.; GRIMSTAD, E. The Q-system following thirty years of development and application in tunneling projects. In: EUROCK, 2004, Salzburg. ***Proceedings*** **[...]**. Essen: VGE Verlag, 2004.

BIENIAWSKI, Z. T. Engineering classification of jointed rock masses. ***Transaction of the South African Institution of Civil Engineers***, v. 15, n. 12, p. 335-343, 1973.

BIENIAWSKI, Z. T. ***Engineering rock mass classifications***: a complete manual for engineers and geologists in mining, civil, and petroleum engineering. New York: John Wiley & Sons, 1989. 272 p.

BRADY, B. H. G.; BROWN, E.T. ***Rock mechanics*****:** for Underground Mining. 3rd. ed. New York: Springer Dordrecht, 2005. 647 p.

BROWN, E. T.; HOEK, E. Trends in relationships between measured in-situ stresses and depth. ***International Journal of Rock Mechanics and Mining Sciences & Geomechanics Abstracts***, v. 5, n. 4, p. 211-215, 1978.

CELADA, B.; TARDAGUILA, I; VARONA, P.; RODRIGUEZ, A.; BIENIAWSKI, Z. T. Innovating tunnel design by an improved experience-based RMR system. *In*: WORLD TUNNEL CONGRESS – Tunnels for a Better Life, 2014, Foz do Iguaçu, Brazil. ***Proceedings*** **[...]**. São Paulo: CBT/ABMS, 2014. p 1–9.

CLARK, L. M. ***Minimizing dilution in open stope mining with a focus on stope design and narrow vein longhole blasting***. 1998. Thesis (MSc), Department of Mining and Mineral Process Engineering, University of British Columbia, Vancouver, 1998.

CLARK, L.; PAKALNIS, R. An empirical design approach for estimating unplanned dilution from open stope hangingwalls and footwalls. *In*: CANADIAN INSTITUTE OF MINING ANNUAL CONFERENCE, 99., 1997, Calgary. ***Proceedings*** **[...]**. Calgary: CIM, 1997.

DIEDERICHS, M. S.; KAISER, P.K. Tensile strength and abutment relaxation as failure control mechanisms in underground excavations. ***International Journal of Rock Mechanics and Mining Sciences***, v. 36, n. 1, p. 69-96, 1999.

GRIMSTAD, E; BARTON, N. Updating of the Q-System for NMT. *In*: INTERNATIONAL SYMPOSIUM ON SPRAYED CONCRETE, 1., 1993, Fagernes. ***Proceedings*** **[...]**. Oslo: Kompen, Opsahl and Berg: Norwegian Concrete Association, 1993. p. 46-66.

HEFNI, M. A.; ABDELLAH, W. R. E.; AHMED, H. M. Factors influencing stope hanging wall stability and ore dilution in narrow-vein deposits: Part II. ***Geotechnical and Geological Engineering***, v. 38, n. 4, p. 3795–3813, 2020.

HENNING, J. G.; MITRI, H. S. Numerical modelling of ore dilution in blasthole stoping. ***International Journal of Rock Mechanics and Mining Sciences***, v. 44, n. 5, p. 692-703, 2007.

HOEK, E.; BROWN, E. T. ***Underground excavations in rock***. London: Institution of Mining and Metallurgy, 1980. 527 p.

HOEK, E.; CARRANZA-TORRES, C.; CORKUM, B. Hoek-Brown Failure Criterion – 2002 Edition. *In*: NORTH AMERICAN ROCK MECHANICS SYMPOSIUM, 5., 2002, Toronto. ***Proceedings*** **[...]**. Toronto: University of Toronto, 2002. p. 267 - 271.

HUTCHINSON, D. J.; DIEDERICHS, M. S. ***Cablebolting in underground mines***. Richmond: Bitech Publishers, 1996. 416 p.

JING, L.; HUDSON, J. A. Numerical methods in rock mechanics. ***International Journal of Rock Mechanics and Mining Sciences***, v. 39, n. 4, p. 409-427, 2002.

MARTIN, C. D.; KAISER, P. K.; TANNANT, D. D.; YAZICI, S. Stress path and instability around mine openings. *In*: ISRM CONGRESS ON ROCK MECHANICS, 9., 1999, Paris. ***Proceedings*** **[...]**. Rotterdam: Balkema, 1999. p. 311 - 315.

MATHEWS, K. E.; HOEK, E.; WYLIE, D. C.; STEWART, S. B. V. ***Prediction of stable excavation spans for mining at depths below 1,000 m in hard rock mines***. Ottawa: CANMET, 1981. (Canmet Report DSS Serial No. OSQ80-00081).

MAWDESLEY, C.; TRUEMAN, R.; WHITEN, W. Extending the Mathews stability graph for open-stope design. ***Mining Technology***, v. 110, n. 1, p. 27-39, 2001.

MELO, M., PINTO, C. L. L., DUTRA, J. ILDEFONSO G. Potvin stability graph applied to brazilian geomechanic environment. ***REM - Revista Escola de Minas***, v. 67, n. 4, p. 413–419, 2014.

NAPA-GARCÍA, G. F.; CÂMARA, T. R.; TORRES, V. F. N. Development and application of a flexible numerical model to evaluate the safety of room-and-pillar mines. ***REM - International Engineering Journal***. v. 72, n. 1, p. 133-139, 2019.

NICKSON, S. D. ***Cable support guidelines for underground hard rock mine operations***. 1992. Thesis (MSc) - Department of Mining and Mineral Processing, University Of British Columbia, Vancouver, 1992.

PARISEAU, W. G. Finite element applications in mining engineering. In: HUDSON, J. A. (ed.). ***Comprehensive rock engineering***. London: Pergamon Press, 1993. v. 1, p. 491-522.

POTVIN, Y. ***Empirical open stope design in Canada***. 1988. Thesis (PhD) - Department of Mining and Mineral Processing, University Of British Columbia, Vancouver, 1988.

ROCSCIENCE. ***RS3***: 3D Geotechnical Finite Element Analysis. Version 4.020. [Toronto]: Rocscience, 2021.

SANTOS, A. E. M.; AMARAL, T. K. M.; MENDONÇA, G. A; SILVA, D. F. S. Open stope stability assessment through artificial intelligence. ***REM - International Engineering Journal***, v. 73, n. 3, p. 395-401, 2020.

SCOBLE, M. J.; MOSS, A. Dilution in underground metal mining: implications for grade control and production management. *In*: WHATELEY, M. K. G.; HARVEY, P. K. (ed.). ***Mineral resource evaluation II***: methods and case histories. London: The Geological Society, 1994. p. 95-108. (Geological Society London - Special Publications, n. 79).

SHEOREY, P. R. A theory for in-situ stresses in isotropic and transversely isotropic rock. ***International Journal of Rock Mechanics and Mining Sciences & Geomechanics Abstracts***, v. 31, n. 1, p. 23-34, 1994.

WANG, J. ***Influence of stress, undercutting, blasting and time on open stope stability and dilution***. 2004. Thesis (PhD) - Department of Civil and Geological Engineering, University of Saskatchewan, Saskatoon, 2004.

ZHU, W.; WANG, P. Finite element analysis of jointed rock masses and engineering application. ***International Journal of Rock Mechanics and Mining Sciences & Geomechanics Abstracts***, v. 30, n. 5, p. 537-544, 1993.

ZINGANO, A. C.; KOPPE, J. C.; COSTA, J. F. C. L. Barrier pillar between production panels in coal mine. ***REM - Revista Escola de Minas***, v. 60, n. 2, p. 219–226, 2007.

Received: 26 November 2021 - Accepted: 25 June 2022.